

Chemical Reaction Dynamics within Anisotropic Solvents in Time-Dependent Fields

Eli Hershkovits* and Rigoberto Hernandez
Center for Computational Molecular Science and Technology
School of Chemistry and Biochemistry
Georgia Institute of Technology
Atlanta, GA 30332-0400[†]
(Dated: July 12, 2018)

The dynamics of low-dimensional Brownian particles coupled to time-dependent driven anisotropic heavy particles (mesogens) in a uniform bath (solvent) have been described through the use of a variant of the stochastic Langevin equation. The rotational motion of the mesogens is assumed to follow the motion of an external driving field in the linear response limit. Reaction dynamics have also been probed using a two-state model for the Brownian particles. Analytical expressions for diffusion and reaction rates have been developed and are found to be in good agreement with numerical calculations. When the external field driving the mesogens is held at constant rotational frequency, the model for reaction dynamics predicts that the applied field frequency can be used to control the product composition.

I. INTRODUCTION

The stochastic or Brownian motion of a particle in a uniform solvent is generally well-understood.^{1,2} The dynamics is less clear when the solvents respond in a non-uniform or time-dependent manner, although such problems are not uncommon. For example, the dynamical properties of a suspension in a liquid crystal can be projected onto an anisotropic stochastic equation of motion.^{3,4} Other examples may include diffusion and reaction in supercritical liquids,⁵ liquids next to the liquid vapor critical point^{6,7,8} and growth in living polymerization.⁹

The flow properties of liquid crystals have generally been analyzed from the perspective of macroscopic nematohydrodynamics.¹⁰ Therein, liquid crystals have been classified according to the presence or absence of solvent. Pure liquid crystals containing no solvent are called thermotropic in part because they have exhibited strong temperature-dependent behavior. A suspension of nematogens (anisotropic molecules) within a simple solvent is known as a lyotropic liquid. The presence of nematogens leads to different transport properties within the solvent than would be seen in a pure simple liquid alone. The additional complexity is a result of the coupling between the velocity field and the average direction of the nematogens. As a result, the dynamics of a particle in the liquid crystal is dissipated by a friction whose form is that of a tensor and not a scalar.¹¹ The actual drag can be further complicated by the presence of topological discontinuities in the liquid.¹² To our knowledge, analytic solutions for the diffusion of Brownian particles in these general environments are not known. The situation for a reactive solute is even less clear as no analytic formalism has been constructed. In the present work, we construct a formalism—that in some limits—fills in these gaps.

One step toward understanding the dynamics in anisotropic liquids would thus be the development of a lyotropic model consisting of a Brownian particle in the

presence of a time-dependent driven mesogen.¹³ Another step toward this goal is the analytic and/or numerical solution of such. In the present work, the rigorous construction necessary for the first of these steps is not attempted. Instead, a naive phenomenological model describing the dynamics in lyotropic liquids has been constructed. It serves as a benchmark for the development of techniques useful in analyzing the dynamics of Brownian particles dissipated by an anisotropic solvent through a time-dependent friction. In particular, the lyotropic liquid is assumed to be nematic, *i.e.*, the (calamitic) mesogens are assumed to be rod-like as is the case with mineral moieties in water¹⁴. The mesogens are further assumed to be one-dimensional and rigid, and a series of additional simplifying assumptions have been invoked. A physical system rigorously satisfying all these assumptions may not exist, but the benchmark may still exhibit some of the important dynamics that has been seen in real liquid crystals in the presence of magnetic fields with time and space instabilities.¹⁵ Another step toward understanding the dynamics in anisotropic liquids is the rigorous solution of a thermotropic (nematic) model in which the dilute Brownian particle diffuses or isomerizes in a solvent that consists exclusively of mesogens. It is based on the possible connection to a rotating nematic liquid system previously observed,^{16,17} and on the analytic understanding of the dynamics in nematic liquids in a few special cases.^{11,18} For this thermotropic case, we don't attempt to develop a microscopic model of the friction and instead make assumptions based on the known properties of isotropic liquids.

In general, the complicated microscopic dynamics of a subsystem coupled to a many-dimensional isotropic heat bath can be projected onto a simple reduced-dimensional stochastic equation of motion in terms of the variables of the subsystem alone. In the limit when the fluctuations in the isotropic bath are uncorrelated, the equation of

motion is the Langevin Equation (LE),¹

$$\dot{q} = p \quad (1a)$$

$$\dot{p} = -V'(q) - \gamma p + \xi(t). \quad (1b)$$

where (q, p) are the position and momenta vectors in mass-weighted coordinates (*i.e.* mass equals one), $V(q)$ is the system potential, γ is the friction and ξ is a Gaussian random force due to the thermal bath fluctuations. The friction and the random force are connected via the fluctuation dissipation theorem,

$$\langle \xi(t_1)\xi(t_2) \rangle = \frac{2\gamma}{\beta} \delta(t_1 - t_2), \quad (2)$$

where the average is taken over all realizations of the forces at the inverse temperature $\beta [\equiv (k_B T)^{-1}]$. The LE can represent the generic problem of the escape rates of a thermally activated particle from a metastable well when the thermal energy is much lower than the barrier height.² The one-dimensional LE has been solved in the asymptotic limits of weak and strong friction by Kramers.² A general solution for weak to intermediate friction was found by Melnikov and Meshkov.¹⁹ This result was subsequently extended to the entire friction range in the turnover theory of Pollak, Grabert and Hänggi.²⁰ The reactive rates for a multidimensional LE have been obtained exactly in the strong^{21,22,23,24,25,26} and weak friction²⁴ limits and approximately in between these limits through a multidimensional turnover theory.²⁷ The LE can also describe the dynamics of a subsystem under an applied external force, and has led to the observation of such interesting phenomena as stochastic resonance,^{28,29} resonant activation,^{30,31} and rectified Brownian motion.^{32,33,34,35}

When the fluctuations in the isotropic bath do not decay quickly in space or in time, the dynamics are known to be described by the the Generalized Langevin Equation (GLE).³⁶ The activated rate expression for a particle described by a GLE is also well-known.^{37,38} Less understood are the exact rates when the friction dissipates the subsystem differently at different times in a nonstationary GLE-like equation.^{5,9,13,39,40,41} Nonetheless, the models developed in this work contain the flavor of this nonstationarity in that the LE is driven by an external periodic field through the friction rather than through a direct force on the system. Consequently the result of this study also provide new insight into the dynamics of systems driven out of equilibrium.

The primary aim of the paper is the development of analytical and numerical techniques to obtain the diffusion and reaction rates of a subsystem dissipated by a time-dependent driven anisotropic solvent in various limits. A naive model for a nematic lyotropic liquid and its various underlying assumptions is presented in Sec. II as one paradigmatic example for the accuracy of the methods described in this work. Another model based on an experimental system of the rotating nematic liquid is described briefly in Sec. III. The anisotropic solvent is

manifested in these models by way of a time-dependent friction that is externally driven. The diffusion of free Brownian particles dissipated by a time-dependent environment is described in Sec. IV. The numerical methods for calculating reactions rates needed to extend the solutions of these models to include nontrivial potentials of mean force are presented in Sec. V A. Analytical approximations for otherwise-rigorous rate formulas are derived and compared to the the numerical results in Sec. V B. A discussion of the validity of all of these approaches and possible applications concludes the paper in Sec. VI.

II. A NAIVE LYOTROPIC MODEL WITH ROTATING EXTERNAL FIELDS

A naive model describing a particle propagated in an anisotropic solvent is motivated in this section in the context of diffusive or reactive dynamics within a lyotropic solvent. The connection between the model and realizable lyotropic solvents is only a loose one. No attempt is made here to do a rigorous projection of the detailed complex modes of the lyotropic solvent onto the subsystem dynamics. The lyotropic liquid is assumed to consist of rod-like mesogens and a uniform isotropic liquid solvent. It is further assumed that there exists a single tagged motion characterized by an effective coordinate q that describes the subsystem — *e.g.*, a probe particle or reacting pair of particles — whose dynamics is of interest. This tagged motion is taken to be one-dimensional for simplicity. The effective mass m_q associated with the tagged subsystem is also assumed to be well separated from the smaller mass of the isotropic liquid, and the larger mass of the (anisotropic) rod-like mesogens. Consequently the tagged motion can be described as that of a Brownian particle at position q experiencing a dissipative environment due to the interactions with the isotropic liquid and the mesogens.

The model is further simplified by assuming that the mesogens of given concentration, c , do not interact with each other. This ideal-solute assumption is certainly realized at low enough concentrations that the mean spacing between mesogens is long compared to their effective interaction distance. (It would be easy to achieve such concentrations even at relatively high concentrations if the interaction potentials are hard-core.) The ideal-solute mesogens will exhibit no orientational order in the absence of external fields.

In real nematic liquids there are interactions between the mesogens that result from cooperative forces. They, as well as boundary effects on the rods, are excluded within the model of this work. The orientation of all the rods is firmly fixed by a magnetic field (homogeneous director field) with inclination θ relative to the y axis:

$$H_x = H_0 \sin \theta \quad (3a)$$

$$H_y = H_0 \cos \theta \quad (3b)$$

$$H_z = 0, \quad (3c)$$

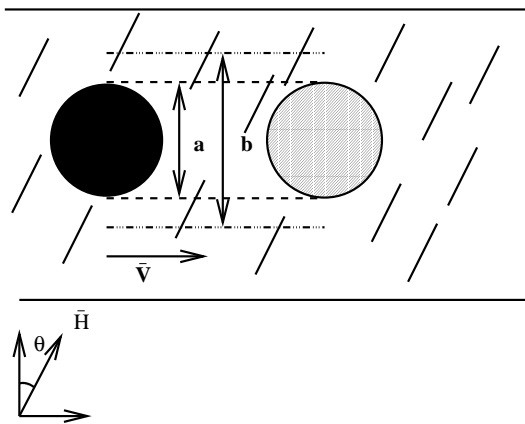


FIG. 1: A Brownian particle with a diameter $2a$ moves with velocity \vec{v} inside a mixture of an isotropic liquid and calamitic mesogens. The mesogens have a length l of the same order of a , a negligible width and concentration, c . The mesogens are oriented by an external magnetic field \vec{H} . The magnetic field is characterized by the angle θ relative to \vec{v} . Under these conditions, the Brownian particle collides with $(\pi R^2 + 2Rl|\cos\theta|)$ mesogens per unit time.

This strong field assumption—all the mesogens will orient uniformly in the direction of \vec{H} —also ensures that there is no angular momentum transfer in collisions between the mesogens and diffusing Brownian solutes. The environment is clearly anisotropic, and a Brownian particle diffusing through it would experience different dissipative forces depending on the direction of its motion. The suspended particle is assumed to have a spherical shape with a radius R . The particle velocity $v(t)$ is restricted to the x direction. The number of collisions per unit time between the Brownian particle and the mesogens is simply $(\pi R^2 + 2Rl|\cos\theta|)vc$. This result is illustrated in Fig. 1. Further assuming that each of the mesogens has a thermal distribution of velocities and noting the mass difference between the mesogens and the environment, the friction force on the Brownian particle is proportional to the number of collisions. This gives a friction coefficient:

$$\gamma = \gamma_0(\pi R^2 + 2Rl|\cos\theta|), \quad (4)$$

where γ_0 is a proportionality constant characteristic of the system. The viscosity of the isotropic liquid leads to additional dissipation that is manifested as an additional constant term to the overall friction. However, in those cases when this isotropic friction is dominated by the friction of Eq. 4, its effect is small and insufficient to blur the anisotropy of the system. For further simplicity, therefore, in what follows, the isotropic friction due to the homogeneous solvent will be assumed to be zero without loss of generality as long as the actual isotropic friction is weak in this sense.

The instantaneous inclination $\theta(t)$ has a large influence on the short-time dynamics of a particle whose motion is measured only along an initially chosen x axis. Without

this restriction, a fixed θ will not influence the dynamics because the particle motion will necessarily average over all directions. As a result, the inclination can be used as a control parameter when one measures only the dynamics along a specific direction but not when one is interested in the average diffusion or reaction of the chosen subsystem with respect to all directions.

In cases when the magnetic field of Eq. 3 rotates with frequency ω , then the Brownian particle experiences a friction,

$$\gamma(t) = \gamma_0(\pi R^2 + 2Rl|\cos\omega t|), \quad (5)$$

that is periodic in time. Including the dissipation of the rotating mesogens will not change this friction, but will add a finite temperature to the bath due to rotational dissipation. As long as this amount of heat is much smaller than the bath temperature, the friction in Eq. 5 is well-defined and can be used as the friction entirely dissipating the Brownian particle.

III. A NEMATIC MODEL WITH EXTERNAL ROTATING FIELDS

While the naive model described above does capture some of the features of liquid crystal diffusion, it is nonetheless too simplistic. Experiments of pure nematic liquids under a rotating magnetic field^{16,17} can serve to illustrate the possibility of solvent responses characterized by time dependent viscosity. In these experiments, the homogeneous director field of a nematic liquid confined between two parallel glass plates was aligned in the plane of the plates by strong magnetic field. The magnetic field was also rotated at constant velocity within this plane. For many of the experimental conditions, the nematic liquid retained uniform alignment but its homogeneous director field followed the magnetic field with a constant phase lag. Finding an expression for the viscosity in a nematic liquid is far more complicated than for an isotropic liquid. It has five coefficients¹⁰ and depends on the orientation of the director, the velocity and the velocity gradient. This problem was only partially solved for some special cases. One case obtains the effective viscosity in a suspension of small particles in a nematic liquid.¹⁸ The key simplifications are that the small particles are assumed to be not much larger than the nematogens and with spherical shape. The friction coefficient has the simple form,

$$f_i = a(A\delta_{ik} + B\cos^2\theta), \quad (6)$$

where the expression for constant coefficients A and B may be found in Ref. 18. A second case treats the limit in which the chosen particle in a nematic liquid has a large spherical shape.¹¹ The resulting effective friction is composed of an isotropic term and an anisotropic term that depends on the angle between the director and the particle velocity. The anisotropic expression is a little

more complicated than Eq. 6, but its leading order terms also involve $\sin \theta$ and $\cos \theta$. In both of these cases, the nematic liquid is assumed to be firmly oriented by a strong external field and the friction force is taken to be much larger than the elastic forces in the nematic liquid. Thus the naive model described in the previous section does exhibit both a uniform constant term and an anisotropic oscillatory term that are in qualitative—though not quantitative—agreement with more detailed models.

IV. FREE BROWNIAN DIFFUSION IN AN ANISOTROPIC SOLVENT

The motion of a free Brownian particle in the time-dependent friction field of Eq. 5 can be described by the Langevin equation,

$$\dot{p} = -\gamma_0 \phi(t)p + \psi(t)\xi(t), \quad (7)$$

where the time-dependent coefficients,

$$\phi(t) = \psi(t)^2 \quad (8a)$$

$$\psi(t) = a + \cos(\omega t), \quad (8b)$$

have been chosen to describe the periodic behavior of the naive lyotropic model and the hydrodynamical friction terms in pure nematics as simply as possible. The noise is related to the friction by the fluctuation dissipation relation,

$$\langle \xi(t)\xi(t') \rangle = \frac{2\gamma_0}{\beta} \delta(t-t'). \quad (9)$$

The strength a of the isotropic term has been chosen to be 1.05 throughout the illustrations in this work to emphasize the anisotropic effects, but different physically-realizable strengths do not lead to different conclusions.

The solution to the equation of motion 7 is

$$p(t) = p_0 \exp[-\gamma_0 G(t)] + \int_{t_0}^t dt_1 \psi(t_1) \xi(t_1) e^{-\gamma_0 \{G(t) - G(t_1)\}}, \quad (10)$$

where p_0 and t_0 satisfy the initial condition, $p_0 \equiv p(t_0)$, and the integrated friction $G(t)$ is defined as

$$G(t) = \int_{t_0}^t dt_1 \psi(t_1)^2. \quad (11)$$

The velocity correlation function is readily calculated to be

$$\langle p(t_1)p(t_2) \rangle = \frac{1}{\beta} \exp[-\gamma_0 \{G(t_1) + G(t_2) - 2G(\min(t_1, t_2))\}]. \quad (12)$$

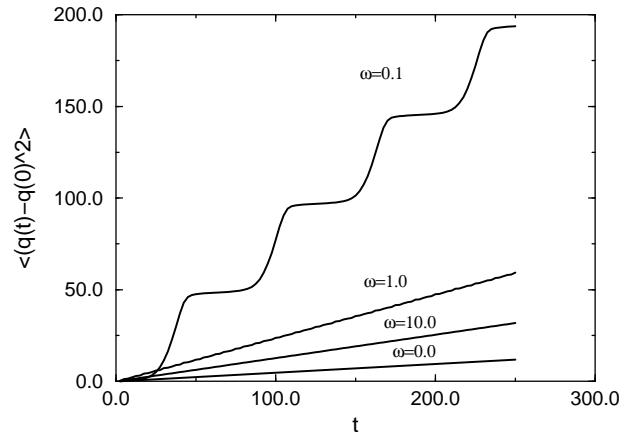


FIG. 2: The mean square displacement of a free Brownian particle in the naive lyotropic bath model has been obtained by direct integration and through the use of the analytical expression in Eq. 13 at various frequencies ω of the driving rotating magnetic field. In the former integration method, 100,000 trajectories were sufficient to obtain convergence. In the latter, the average is taken over an ensemble of 100,000 particles starting at time $t = 0$ with inclination perpendicular to the velocity, and overlays the results of the former within the resolution of the figure.

The square mean displacement of the free particle after time t is the double integral,

$$\begin{aligned} \langle (q(t) - q(t_0))^2 \rangle &= \int_{t_0}^t \int_{t_0}^t dt_1 dt_2 \langle p(t_1)p(t_2) \rangle \end{aligned} \quad (13a)$$

$$\begin{aligned} &= \frac{1}{\beta} \left[\int_{t_0}^t dt_1 \int_{t_0}^{t_1} dt_2 e^{-\gamma_0 \{G(t_1) - G(t_2)\}} \right. \\ &\quad \left. + \int_{t_0}^t dt_1 \int_{t_1}^t dt_2 e^{\gamma_0 \{G(t_1) - G(t_2)\}} \right]. \end{aligned} \quad (13b)$$

A similar expression was developed by Drozdov and Tucker⁵ for the case of fluctuations in the local density of supercritical solvent. The result in Eq. 13 leads to the diffusivity of the particle. As will be shown below, the diffusivity in the time-dependent environment deviates from the linear correlation known to result in the constant friction environment.

In Fig. 2, the mean square displacement of a Brownian particle whose motion is measured only along an arbitrary one-dimensional axis is plotted as a function of time at various applied frequencies ω . The *average behavior* of the mean square displacement is linear with time, as in the constant friction regime, but it also contains fluctuations (in time) around the average whose frequency depends on the external field. It is important to note that the overall slope of the mean square displacement depends on the frequency ω ; that is, the diffusivity shows strong dependence on ω . Hence by changing the

frequency of the external field, it becomes possible to control the diffusivity of the Brownian particles.

The analytical result of Eq. 13 was used to check the accuracy of the numerical integrator employed in propagating particles in a time-periodic white noise bath. A fourth-order integrator was developed based on the Taylor method in Refs. 13 and 42 and is outlined in Appendix A. Such an algorithm is extremely useful as a check for nonstationary problems in which the integration time can be very long. The new algorithm agrees with the analytical result up to time steps of size, $\delta t = .5$, in the dimensionless units of time defined in Eq. 7. In general, the time step required to achieve a given accuracy decreases as either the frequency or friction increases.

These results are limited to diffusion in one dimension. When studying the motion in the plane defined by the rotating magnetic field an average has to be taken over all the directions. The integrated friction function, Eq. 11, for a particle with the initial velocity inclined with angle $\omega\tau$ relative to the magnetic field at the time, $t = 0$, is

$$G(t + \tau) = \gamma_0 \left[a^2 t + \frac{2a}{\omega} \sin(\omega(t + \tau)) + \frac{t}{2} + \frac{\sin[2\omega(t + \tau)]}{4\omega} \right]. \quad (14)$$

After some elementary algebra, the integration in 13 with G as in Eq. 14 for the case of a constant magnetic field leads to the average diffusion coefficient,

$$\langle D \rangle_0 = \frac{1}{\gamma_0 \beta} \frac{a}{(a^2 - 1)^{3/2}}, \quad (15)$$

of a Brownian particle in a plane. The diffusivity of the Brownian particle in a rotating field at various frequencies has been obtained numerically and is shown in Figure 3. As can be seen, the diffusivity is a monotonic decreasing function of the frequency. This result suggests the use of the applied field frequency to control the diffusive transport of the Brownian particle.

In the $a = 1$ limit of this model, there is a divergence in the averaged diffusion constant over all the directions at constant magnetic field. This limiting behavior is a consequence of a transition from diffusive to ballistic motion at the inclination in which $\theta = \pi$. That is to say, that it is an artifact of the model in so far as the physical system it represents would never take on the value of $a = 1$, and hence would not exhibit an infinite diffusion! Nonetheless, the model above serves to demonstrate the accuracy of the numerical and analytical formalism when a is far from 1.

V. REACTION RATES IN A TIME-PERIODIC FRICTION

The assumptions introduced in Sec. II are also applicable to the description of the reactive interactions between

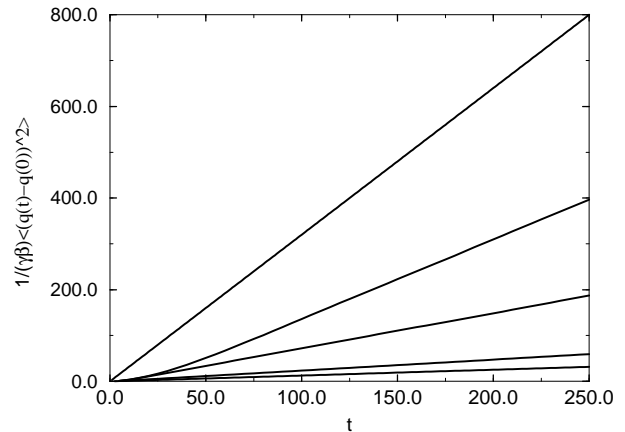


FIG. 3: The normalized average displacement of an ensemble of free Brownian particles in the presence of a periodic friction is displayed as a function of time. The driving frequencies are $\omega = 10, 1, 0.1, 0.2$ and 0. The result for the fixed case ($\omega = 0$) has been calculated analytically using Eq. 15. The remaining results are obtained numerically by averaging over Brownian particles with velocities in random inclination relative to the magnetic field at the initial time, $t = 0$. Note that the slopes—*viz.*, the diffusion rate— increase with decreasing ω .

two Brownian particles. Neglecting the hydrodynamic interaction as before, the dynamics can be described by the time-dependent Langevin equation,

$$\ddot{q} = -\nabla V(q) - \gamma_0 \phi(t) \dot{q} + \psi(t) \xi(t), \quad (16)$$

where q is now a relative mass-weighted coordinate between the interacting particles, and V is the potential of mean force between the particles. The remaining symbols are the same as in the previous section. Phenomenological rate constants—*e.g.*, transition from one metastable state of the potential to another or to infinity—cannot be calculated analytically when the potential is of a more complex form than that of the harmonic oscillator. Direct numerical evaluation of these rates is usually quite time consuming because the time scales involved in the problem are widely varying. The reactive flux method reduces much of the computation time by initiating the trajectories at the barrier.² It has been used to obtain reactive exact thermal escape rates in the stationary limit both numerically and exactly, and to obtain approximate rates under a variety of limiting approximations. In the present case, the problem is nonstationary at short times but retains an average stationarity at sufficiently long times. The strategy is consequently to generalize the rate formula for stationary systems. It must now include processes in which stationarity is required only when the observables are integrated over a period equal to that of the external periodic perturbation.

In all of the calculations performed here to illustrate the approach, the potential has been chosen to have the

the form of a symmetric quartic potential,

$$V(q) = q^4 - 2q^2, \quad (17)$$

in which the two minima represent two distinct metastable states separated by a dimensionless barrier of unit height. (Note that for simplicity, all observables in this work are written in dimensionless units relative to the choice of this effective barrier and the particle mass.) The reactive rate has been calculated for particles with inverse temperatures, $\beta = 10$, or 20. These temperatures are low enough to give a well-defined phenomenological rate when the reactive flux method is employed in the constant friction case, but not so low that trajectories are needlessly slow even when one obtains the rate by direct methods.

A. Rate Formula and Numerical Methods

The standard approach for calculating reaction rates, “the reactive flux method,” assumes stationarity.^{2,43} In establishing its validity, the rate formula needs to be checked by comparison with direct methods measuring the phenomenological rates between reactants and products. In this section, a direct approach for obtaining rates in the nonstationary cases of interest to this work is reviewed and similarly validated. The results of this approach are subsequently used to motivate an averaged reactive flux formula appropriate for the nonstationary case.

In the direct approach, one simply calculates the rate of population transfer from the reactant population n_a to the the product population n_c . The initial population is assumed to be thermally distributed entirely at the reactant side. The latter assumption is valid because the Boltzmann distribution is the steady state solution of the system restricted to the reactant region (App. B). Assuming that a simple first-order master equation describes the rate process (App. B), the population in the reactant well can be solved directly as,

$$\frac{n_a(t) - \bar{n}_a}{n_a(t_0) - \bar{n}_a} = \exp\left(-\int_{t_0}^t dt' \lambda'(t')\right), \quad (18)$$

where the relaxation rate $\lambda(t) = k^+ + k^-$ is the sum of the forward (k^+) and reverse (k^-) rates, \bar{n}_a is the population in the left well at equilibrium. At equilibrium, for a symmetric potential, $n_a(t) = n_c(t) = N/2$, where N is the total population of Brownian particles. In a nonequilibrium bath, such as is seen in the model described in Sec. II, that has oscillatory components with a maximum recurrence time, then a phenomenological rate may still be obtained by averaging at sufficiently long times compared to the maximum recurrence time. In particular,

$$\bar{\lambda}^{(1)} \equiv \frac{1}{t - t_0} \int_{t_0}^t \lambda(t') dt' \quad (19a)$$

$$= -\frac{1}{t - t_0} \ln \left[\frac{n_a(t) - N/2}{N/2} \right]. \quad (19b)$$

The second equality was introduced by Pollak and Frishman⁴⁴ as a construction that can lead to long time stability thereby ensuring a substantial plateau time.⁴³ The instantaneous flux can be found using the differential expression⁴⁴:

$$-\lambda(t) = \frac{1}{n_a - n_c} \frac{d}{dt} (n_a - n_c) \quad (20a)$$

$$= \frac{d}{dt} \ln (n_a - n_c). \quad (20b)$$

The numerical calculation of either of the direct rate formulas requires the direct integration of a large number of trajectories all initiated in the reactant region. Consequently, it will only be accurate when the numerical integrator is accurate for times that are sufficiently long to capture the rate process. This holds at the moderate temperatures (near $\beta V^\ddagger = 10$) explored in this work for which Eqs. 19 and 20 lead to the same result. The first method was used in all of the direct calculations in this work because it tends to be more stable.

The direct methods are time consuming and it is practically impossible to apply them at low temperatures. As was mentioned at the beginning of this section, the typical solution of this problem is the use of the reactive flux method. It samples only those states that traverse the dividing surface. For stationary systems, the reactive flux is²

$$k^+ = \frac{\langle \delta[q(0)] \dot{q}(0) \theta[q(t)] \rangle}{\langle \theta(q) \rangle}, \quad (21)$$

where the characteristic equation $\theta[q(t)]$ for a trajectory is 1 if the particle is in the right well at time t and zero otherwise, and the Dirac δ -function ensures that all the particles are initially located at the barrier (at $x = 0$). The angle brackets represent the averaging over the thermal distribution of the initial conditions.

One might naively assume that the rate expression in Eq. 21 might still hold in the nonstationary case of time periodic friction, Eq. 8. The direct and reactive-flux rates at different frequencies and different friction constants are compared in Table I. The two don't always agree and the difference can be as much as an order of magnitude. This result should not be surprising because of the nonstationarity of the problem. However, correlation functions for this system do become stationary when one averages over the period of the external perturbation. This suggests that Eq. 21 should be further averaged over the initial time during a period of the external field, yielding the average reactive flux rate,

$$\bar{\kappa}(t) = \frac{\omega}{2\pi} \int_0^{\frac{2\pi}{\omega}} d\tau \frac{\langle \delta[x(\tau)] \dot{x}(\tau) \theta[x(t + \tau)] \rangle}{\langle \theta \rangle}. \quad (22)$$

Rates at $\gamma = 10$	ω			
	0	0.1	1	10
integral method	2×10^{-6}	1.17×10^{-5}	1.55×10^{-5}	8.5×10^{-5}
reactive flux	2×10^{-6}	2×10^{-6}	2×10^{-6}	2.3×10^{-6}
Rates at $\gamma = 1$	ω			
	0	0.1	1	10
integral method	1.7×10^{-5}	2.2×10^{-5}	2.9×10^{-5}	3×10^{-5}
reactive flux	1.6×10^{-5}	1.6×10^{-5}	1.6×10^{-5}	2.5×10^{-5}
Rates at $\gamma = 0.05$	ω			
	0	0.1	1	10
integral method	3.3×10^{-5}	1.55×10^{-5}	1.47×10^{-5}	2.05×10^{-5}
reactive flux	3×10^{-5}	3.15×10^{-5}	1.76×10^{-5}	1.9×10^{-5}

TABLE I: The integral method of Eq. 19 is compared to the stationary reactive flux method of Eq. 21 in calculating the activated rate across the double-well potential in a rotating field of frequency ω . All the calculations are performed at the same bath temperature such that $\beta V^\ddagger = 10$, and at three different values of γ illustrative of the low, intermediate and high friction limits. Here and elsewhere, all values are reported in the dimensionless units of Eq. 16.

(There is a formal proof in Appendix B.) A comparison between the direct rates and the average reactive flux rate is presented in Table II. The numerics were performed at a temperature ($\beta V^\ddagger = 10$) that is high enough to enable direct calculation of the rate within a few hours of CPU time on a current workstation. As can be seen from the table, there is very good agreement between the methods. Equation 22 is the central result of this article, and represents the fact that *the reactive flux method is valid for the case of a time-dependent bath when a proper averaging is taken over the period of the external field*. This result is critical for the numerical calculation of rates because the direct approaches are cost prohibitive when the temperature is much smaller than barrier height. In this section the reactive flux method has been generalized to include out-of-equilibrium systems in cases in which an external force perturbs a bath that is coupled to a reactive system. The resulting thermal flux is defined only after averaging over the time period of the external perturbation. Using the non averaged rate expression would lead to undefined rates because the reactive system is so far out of equilibrium. A detailed explanation can be found in App. B.

B. Analytical Approximations

1. Weak Friction

For the stationary problem, Melnikov and Meshkov¹⁹ developed a perturbation technique to find the reactive flux at weak to moderate friction limit.²⁰ The expansion parameter of the method is the energy loss δ that a particle starting at the barrier experiences while traversing

the well. Its value is

$$\delta = \gamma \beta s, \quad (23)$$

where s is the action of a frictionless particle starting with zero momentum at the barrier and returning back to the top of the barrier after traversing a periodic orbit (the instanton), *i.e.*,

$$s = \int_{-\infty}^{\infty} p^2(t) dt = \int_{q(-\infty)}^{q(\infty)} p dq. \quad (24)$$

The resulting rate is

$$k = k_{\text{TST}} \Upsilon, \quad (25)$$

where $k_{\text{TST}} = \frac{\omega}{2\pi} e^{-\beta V^\ddagger}$ is the transition state theory rate (ω is the frequency at the bottom of the reactant well and V^\ddagger is the barrier height) and the depopulation factor Υ is

$$\Upsilon(\delta) = \exp \left\{ \frac{1}{2\pi} \int_{-\infty}^{\infty} \ln \left[1 - e^{\delta(\lambda^2 + 1/4)} \right] \frac{1}{\lambda^2 + 1/4} d\lambda \right\} \quad (26)$$

The nonstationary analytic rate expression can now be obtained by analogy to the formulation of the average reactive flux rate in which the rate is averaged over the period of driving term. In particular, the energy loss,

$$\delta(\tau) = \gamma \beta \int_{-\infty}^{\infty} \psi(t + \tau)^2 p^2(t) dt, \quad (27)$$

is now obtained as a function of the possible initial configurations of the driving term which are, in turn, parameterized by the time lag τ relative to the start of an oscillation in the friction of Eq. 8. Trajectories in one dimension can be calculated up to a quadrature directly from energy conservation,

$$q(t) = q(t_0) + 2 \int_{t_0}^t dt \sqrt{E - V(q)}. \quad (28)$$

In the case of the double-well potential defined by Eq. 17, the instanton at $E = V^\ddagger$ —*viz.* the periodic orbit on the upside-down potential— can be obtained analytically. The results for time,

$$t(q) = -\frac{1}{2} \ln \left(\frac{\sqrt{2} + \sqrt{2 - q^2}}{q} \right), \quad (29)$$

and momentum,

$$p(q) = \sqrt{2} q \sqrt{2 - q^2}, \quad (30)$$

as a function of q follow readily. By substitution into Eq. 27, the energy loss parameter is obtained directly with respect to the time lag τ relative to the start of an oscillation in the friction of Eq. 8, *i.e.*,

$$\begin{aligned} \delta(\tau) = & 2\gamma\beta \int_0^{\sqrt{2}} dq \left\{ a \right. \\ & \left. + \cos \left[-\frac{\omega}{2} \ln \left(\frac{\sqrt{2} + \sqrt{2 - q^2}}{2} \right) + \omega\tau \right] \right\} \\ & \times \sqrt{2} q \sqrt{2 - q^2}. \end{aligned} \quad (31)$$

ω	γ					
	.005	.05	.5	1	10	
.1	3 $\times 10^{-6}$ (2.78 $\times 10^{-6}$)	1.55 $\times 10^{-5}$ (1.51 $\times 10^{-5}$)	2.3 $\times 10^{-5}$ (2.3 $\times 10^{-5}$)	2.1 $\times 10^{-5}$ (2.1 $\times 10^{-5}$)	1.15 $\times 10^{-5}$ (1.18 $\times 10^{-5}$)	
.5	2.8 $\times 10^{-6}$ (2.62 $\times 10^{-6}$)	1.43 $\times 10^{-5}$ (1.45 $\times 10^{-5}$)	2.22 $\times 10^{-5}$ (2.23 $\times 10^{-5}$)	2.1 $\times 10^{-5}$ (2.13 $\times 10^{-5}$)	1.375 $\times 10^{-5}$ (1.41 $\times 10^{-5}$)	
1.0	3 $\times 10^{-6}$ (2.7 $\times 10^{-6}$)	1.45 $\times 10^{-5}$ (1.39 $\times 10^{-5}$)	3 $\times 10^{-5}$ (3.01 $\times 10^{-5}$)	2.7 $\times 10^{-5}$ (2.7 $\times 10^{-5}$)	1.45 $\times 10^{-5}$ (1.47 $\times 10^{-5}$)	
5.0	3 $\times 10^{-6}$ (2.7 $\times 10^{-6}$)	1.9 $\times 10^{-5}$ (1.86 $\times 10^{-5}$)	3.25 $\times 10^{-5}$ (3.26 $\times 10^{-5}$)	2.8 $\times 10^{-5}$ (2.86 $\times 10^{-5}$)	1.2 $\times 10^{-5}$ (1.14 $\times 10^{-5}$)	
10.0	3 $\times 10^{-6}$ (2.7 $\times 10^{-6}$)	1.92 $\times 10^{-5}$ (1.92 $\times 10^{-5}$)	3.25 $\times 10^{-5}$ (3.35 $\times 10^{-5}$)	2.7 $\times 10^{-5}$ (2.78 $\times 10^{-5}$)	8.6 $\times 10^{-6}$ (8.87 $\times 10^{-6}$)	

TABLE II: The integral method of Eq. 19 is compared to the average reactive flux method of Eq. 22 in calculating the activated rate across the double-well potential in a rotating field of frequency ω and various friction constants γ . The potential and inverse temperature ($\beta V^\ddagger = 10$) are the same as in Table I. At each entry, the integral method result is written above the more approximate average reactive flux result. To aid the eye, the latter is also signaled by parentheses.

The nonstationary rate formula for a time-periodic driving friction can thus be written as the product of the TST rate and a generalized depopulation factor averaged over τ ,

$$\bar{\Upsilon}[\delta] \equiv \int_0^1 d\tau \Upsilon(\delta(\tau)), \quad (32)$$

in analogy with Eq. 25.

The validity of the analytical result of Eq. 32 for the rate can be checked in the low friction regime in which $\Upsilon(\delta) \approx \delta$. Taking the average over a period yields the result,

$$\begin{aligned} \bar{\Upsilon}[\delta] &\approx \frac{\omega}{2\pi} \int_0^{2\pi/\omega} \delta(\tau) d\tau \\ &= \frac{8}{3} \left(a^2 + \frac{1}{2} \right). \end{aligned} \quad (33)$$

This result is in good agreement with the averaged reactive flux rate formula of Eq. 22, as shown in Table III at a low friction value ($\gamma_0 = .005$), $\beta V^\ddagger = 10$, and various frequencies. Even within this weak friction regime, as the friction increases, the approximation leading to Eq. 33 will break down. The direct evaluation of Eq. 32 corrects this error, and also leads the rate to depend on the frequency of the driven friction.

2. Strong Friction

The reaction rate in the overdamped regime of the LE is well known.² The central idea is that the motion in phase space is strongly diffusive in this regime. The rate is consequently dominated by the dynamics close to the barrier. At the vicinity of the barrier top, the potential can be approximated by an inverted parabolic potential and the LE at the barrier can be written as

$$\ddot{q} = -\omega_b^2 q - \gamma \dot{q} + \xi(t), \quad (34)$$

Rates at $\gamma = 0.005$	ω		
	0.1	1	10
MM (Eq. 33)	8.54 $\times 10^{-2}$	8.54 $\times 10^{-2}$	8.54 $\times 10^{-2}$
$\bar{k}(t)$ (Eq. 22)	7.5 $\times 10^{-2}$	7 $\times 10^{-2}$	7.5 $\times 10^{-2}$

TABLE III: The transmission coefficients for the escape rate k across a quartic potential at $\beta V^\ddagger = 10$ and $\gamma = .005$ obtained using the average reactive flux method of Eq. 22 with the analytical Melnikov-Meshkov expression 33 for $\bar{\delta}$. An ensemble of 100,000 trajectories has been propagated in each of the reactive flux calculations.

where the fixed friction γ and stochastic force $\xi(t)$ satisfy the regular fluctuation dissipation relation (Eq. 2) and $i\omega_b$ is the imaginary frequency at the barrier. It was shown that the reaction rate for this case is^{36,45}

$$k = \frac{\lambda_b}{\omega_b} \frac{\omega_0}{2\pi} \exp(-\beta V^\ddagger), \quad (35)$$

where ω_0 is the frequency of the reactant well, and $i\lambda_b$ is the imaginary eigenvalue of the homogeneous part of Eq.34. The latter is related to the exponential divergence in the trajectories near the barrier,

$$q(t) \propto e^{\lambda_b t}. \quad (36)$$

At strong friction in the nonstationary problem, the reaction rate expression is also dominated by the trajectories in the barrier region. Equation 35 can still be used for the rates, though now $\lambda(t)$ is the time-dependent eigenvalue of the homogeneous part,

$$\ddot{q} + \gamma \phi(t) \dot{q} - \omega_b^2 q = 0, \quad (37)$$

of the nonstationary stochastic equation of motion. The solution of this equation is not trivial. A possible way to solve the problem is found in Ref. 31. It is easier to extract the eigenvalue numerically from the exponential

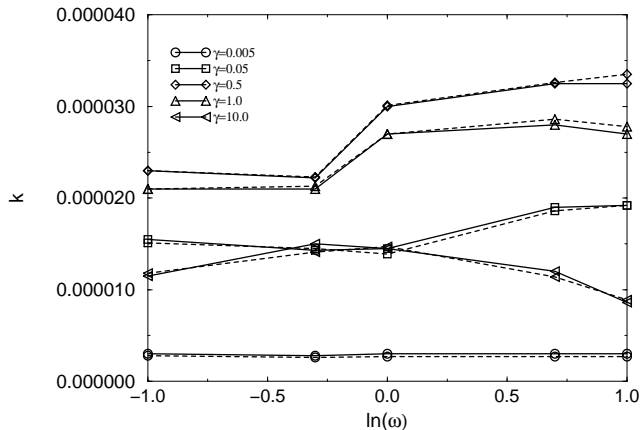


FIG. 4: The activated escape rates k of particles in a quartic potential and solvated by an anisotropic time-dependent liquid is obtained as a function of the driving frequency ω using two numerical methods described in this work. The numerical direct rate of Eq. 19 is shown by dashed lines, and the averaged reactive flux rate of Eq. 22 is shown by solid lines. In the former, an ensemble of 250,000 initial conditions were used to achieve convergence, and the corresponding numerical values are summarized in Table III. In the latter, the average was performed over an ensemble of 100,000 trajectories, yielding the results in a wall-clock time that was an order of magnitude faster than that for the direct rate calculations. In all cases, the inverse temperature βV^\ddagger is 10.

divergence of trajectories starting near the barrier top,

$$q(t) \propto e^{\int^t \lambda_b(t') dt'} . \quad (38)$$

The periodicity of the time dependent coefficient in Eq. 37 leads also to a periodicity in $\lambda_b(t)$. If $\bar{\lambda}_b$ is the time average of the time-dependent eigenvalue of Eq. 37 over a period, then for t much larger than the period, Eq. 38 is analogous Eq. 36 with $\bar{\lambda}_b$ in the exponent. Replacement of λ_b by $\bar{\lambda}_b$ in the rate expression (Eq. 35) provides good agreement with the averaged reactive flux rates as shown in the high friction columns of Table IV.

3. Weak to High Friction

The results of the two previous subsections have motivated the redefinition of the components of the rate formula in the low and high friction limits of the nonstationary time-periodic problem. Retaining these assignments in the stationary turnover rate formula²⁰ suggests the nonstationary turnover rate,

$$\bar{k} = \frac{\bar{\lambda}_b \omega_0}{\omega_b 2\pi} \frac{(\bar{\Upsilon}[\delta])^2}{\bar{\Upsilon}[2\delta]} \exp -\beta V^\ddagger . \quad (39)$$

The prefactors from the nonstationary turnover rate are compared to those from the averaged reactive flux rate at

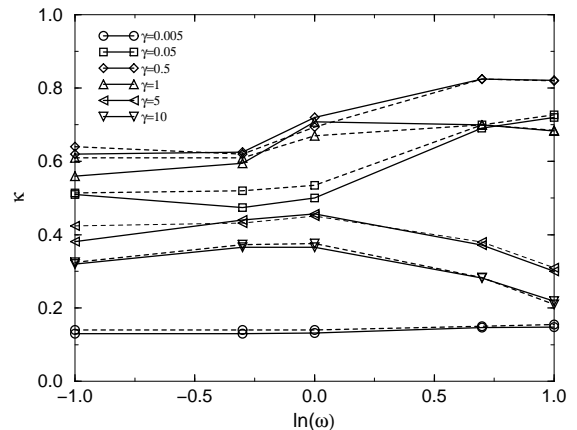


FIG. 5: The activated escape rates k of particles in a quartic potential and solvated by an anisotropic time-dependent liquid is obtained as a function of the driving frequency ω comparing the reactive flux approach to an analytical result. (The latter is expected to be accurate here—and not in Fig. 4 or Table II—because the inverse temperature has been increased to 20.) The solid line corresponds to the numerical result calculated using the averaged reactive flux rate method of Eq. 22 and the dashed line corresponds to the turnover formula in Eq. 39. The numerical calculations were performed by averaging over an ensemble of 250,000 trajectories.

ω	γ					
	.005	.05	.5	1	5	10
.1	(.14)	(.514)	(.64)	(.61)	(.424)	(.325)
	.13	.51	.62	.56	.381	.32
.5	(.14)	(.52)	(.62)	(.61)	(.432)	(.373)
	.13	.474	.625	.595	.44	.366
1.0	(.14)	(.535)	(.694)	(.67)	(.451)	(.376)
	.132	.5	.72	.708	.457	.366
5.0	(.15)	(.7)	(.825)	(.7)	(.38)	(.283)
	.147	.691	.825	.7	.372	.282
10.0	(.155)	(.727)	(.82)	(.685)	(.31)	(.21)
	.148	.720	.821	.683	.3	.219

TABLE IV: The average reactive flux method of Eq. 22 is compared to the analytic approximation of Eq. 39 in calculating the activated rate across the quartic potential in a rotating field of frequency ω and various friction constants γ . The inverse temperature ($\beta V^\ddagger = 20$) is higher in contrast to the previous tables. At each entry, the more approximate average reactive flux result is written above the analytic result. To aid the eye, the former is also signaled by parentheses.

the inverse temperature $\beta = 20$ in Table IV and in Fig. 5. As can be seen, there is a very good agreement between the numerical and analytic results at the very weak and strong friction limits. Therein the results differ by no more than 5% throughout the frequency range; an error margin smaller than the error bars in the numerical

calculations. At moderate friction and low frequencies, however, the differences —on the order of 10%— cannot be explained by error in the numerical calculations alone, and may be significant. Corrections or improvements in the approximations leading to the connection formula of Eq. 39 are also of interest, but not pursued further in this work. Recall that the turnover escape rate expression for the LE with constant friction was obtained through the solution of the equivalent Hamiltonian formalism.²⁰ A similar approach for the solution of a the Hamiltonian equivalent⁴⁶ of the stochastic time-dependent bath problem may lead to a fruitful solution. However, even in the constant friction case, the turnover formula can give rise to small systematic error. With these reservations, the approximate rate formula can be used to obtain time-dependent escape rates. It is clear from the results that there is a frequency effect on the reaction rates. For the specific example studied here, the effect can modify the reaction rate

VI. DISCUSSION AND CONCLUSIONS

In this work, several techniques for obtaining the dynamics of interacting Brownian particles that are coupled to a time dependent thermal bath have been discussed. Two models, one of dynamics in lyotropic liquids and one for dynamics in pure nematic liquid under a periodic external field has been brought as examples of such systems. The models include a new mechanism for stochastic dynamics in which an external force is used to drive the thermal bath. There is no net injection of energy to the Brownian particles in the bath due to the driving force, hence they keep their equilibrium properties. Yet observables such as reaction and diffusion rates are modified. The existence of a steady state that retains the equilibrium enables one to express out-of-equilibrium observables with respect to averaging over the equilibrium. This is the Onsager regression hypothesis (Appendix B). We used this to extend known methods for calculating the reaction rates in the constant friction to nonstationary baths. Extensive computation effort was used to illustrate the diffusive and reactive rates for an effective Brownian particle in the naive anisotropic liquid bath model with rotating magnetic field. However, the numerical and analytical tools that have been modified and developed in this work are appropriate for any model with time-dependent friction.

The construction introduces new control parameters into the problem; namely, the external force amplitude and frequency. We concentrated on the latter and exhibited the frequency dependence of diffusion and reaction rates in the naive model. This dependence is not linear and changes dramatically with the friction strength. The enhancements in the reaction rate and the diffusion coefficient are not the same, *i.e.*, the maximum in the diffusion rate as a function of the external frequency is not the same as the maximum in the rate. This nonlin-

ear behavior could be used to enhance reaction diffusion processes, such as cluster nucleation, by up to a few order of magnitude.

In the extension of the naive model to more realistic nematic liquids, the cooperative effects of the liquid cannot be omitted. There are phenomenological difficulties in defining friction and the fluctuation dissipation relation in liquid crystals. To the best of our knowledge such a theory is still not fully developed. The development of such a theory based on microscopic assumptions is an extremely challenging problem. Boundary effects and elastic forces will create dynamical micro-domains characterized by differing uniform directors in a real nematic under rotating magnetic field. The theory for dynamics in nematics will have to deal also with the spatial inhomogeneities. These are among the challenges to future work in trying to better understand the diffusive dynamics in lyotropic liquids.

ACKNOWLEDGEMENTS

We are grateful to Prof. Rina Tannenbaum for stimulating discussions and helpful suggestions. This work has been partially supported by the National Science Foundation under Grant, Nos. 97-03372 and 02-13223. RH is a Goizueta Foundation Junior Professor. The Center for Computational Science and Technology is supported through a Shared University Research (SUR) grant from IBM and Georgia Tech.

APPENDIX A: FOURTH-ORDER INTEGRATOR FOR THE LE WITH PERIODIC FRICTION

A high-order integrator was developed for the regular LE or GLE in Ref. 42. A modified algorithm for time- and space-dependent friction was developed for the explicit GLE with exponential memory kernel in the friction¹³. This appendix introduces the numerical scheme necessary for solving a time dependent stochastic equation equation of motion of the form of Eq. 7.

A finite difference scheme is used to propagate the solution over a small time step. At each iteration, the propagator is expanded to fourth order with respect to the time step using a strong Taylor scheme.⁴⁷ The resulting integrator can be decomposed into two uncoupled terms:

$$q(t+h) = q_{\text{det}}(p, q, t) + q_{\text{ran}}(p, q, t) \quad (\text{A1a})$$

$$p(t+h) = p_{\text{det}}(p, q, t) + p_{\text{ran}}(p, q, t). \quad (\text{A1b})$$

The deterministic terms that are collected within q_{det} and p_{det} are those that remain in a fourth-order Taylor expansion of the deterministic equation of motion after removing any term that includes a stochastic variable. The deterministic propagator can be calculated numerically with any fourth-order deterministic scheme; the

fourth order Runge Kutta method was chosen for this work.⁴⁸

The random propagator (giving rise to the stochastic contribution, q_{ran} and p_{ran}) includes all terms up to fourth-order that include stochastic variables. For the present case, the random integrator for the space and momenta leads to the contributions,

$$\begin{aligned}
q_{ran} &= a \left\{ \left[\psi + \dot{\psi} + \frac{1}{2} \ddot{\psi} h^2 \right] Z_2 \right. \\
&\quad + \left[-\gamma \psi^3 - 2\dot{\psi} - (2\ddot{\psi} + 3\gamma \psi^2 \dot{\psi}) h^2 \right] Z_3 \\
&\quad \left. + \left[-V'' \psi + \gamma^2 \psi^5 + 2\ddot{\psi} + 7\gamma \psi^2 \dot{\psi} \right] Z_4 \right\} \quad (\text{A2}) \\
p_{ran} &= a \left\{ \left[\psi + \dot{\psi} + \frac{1}{2} \ddot{\psi} h^2 + \frac{1}{6} \psi^{(3)} h^3 \right] Z_1 \right. \\
&\quad + \left[-\gamma \psi^3 - \dot{\psi} - (\ddot{\psi} + 3\gamma \psi^2 \dot{\psi}) h \right. \\
&\quad \left. - \left(-\frac{1}{2} \psi^{(3)} + \gamma(3\psi \dot{\psi}^2 + \frac{3}{2} \psi^2 \ddot{\psi}) \right) h^2 \right] Z_2 \\
&\quad + \left[-V'' \psi + \gamma^2 \psi^5 + \ddot{\psi} + 4\gamma \psi^2 \dot{\psi} \right. \\
&\quad + (p^0 V''' \psi + 5\gamma^2 \psi^4 \dot{\psi} + 4\gamma(2\psi \dot{\psi}^2 + \psi^2 \ddot{\psi}) \\
&\quad \left. - V'' \dot{\psi} + \psi^{(3)}) h \right] Z_3 \\
&\quad \left. + \left[2\gamma V'' \psi^3 - \gamma^3 \psi^7 + p_0 V''' \psi + 3V'' \dot{\psi} - \psi^{(3)} \right. \right. \\
&\quad \left. \left. - 9\gamma^2 \psi^4 \dot{\psi} - 4\gamma(2\psi \dot{\psi}^2 + \psi^2 \ddot{\psi}) \right] Z_4 \right\}, \quad (\text{A3})
\end{aligned}$$

where $\psi(t)$ is the coefficient in Eq. 8 dictating the time-dependence in the friction, and the Gaussian random variables $\{Z_i\}$ are correlated according to the moments specified in Ref. 42. The symbol, $\psi^{(3)}$, with the parenthesized superscript, denotes the third-order derivative of ψ with respect to time. There is frequent repetition of terms differing by no more than a ratio of constant coefficients, and this allows the integrator to be computed very economically despite the seemingly large number of terms contained above. In fact, the most time-consuming part of the scheme is the calculation of the random numbers. Although the fourth-order integrator has been expanded in terms of the stochastic variables, the neglected higher-order terms have coefficients that depend on the friction and frequencies to high order. Consequently, the algorithm loses its efficiency at high friction or in the high frequency domain. For a given problem, a comparison of the fourth-order algorithm to lower-order algorithms such as the velocity Verlet algorithm⁴⁹ is advisable to ensure that the requisite accuracy is achieved. Though not presented explicitly here, such comparisons have been performed with favorable agreement for the models of this work. The fourth-order integrator is accurate, and equally importantly, provides a substantial savings in computational time.

APPENDIX B: REACTIVE FLUX METHOD FOR SYSTEMS IN NONSTATIONARY ENVIRONMENT

The reactive flux formalism is an efficient numerical tool for calculating the escape rates of Brownian particle from a metastable well at low temperatures. The derivation of the reactive flux method is well formulated.² In this appendix, the derivation is recapitulated in order to emphasize the new considerations that emerge because of nonstationarity. The corner stone for any rate calculation in a nonequilibrium system is “the Onsager regression hypothesis.”⁵⁰ This hypothesis asserts that “the relaxation of macroscopic non-equilibrium disturbances is governed by the same laws as the regression of spontaneous microscopic fluctuations in an equilibrium system.”⁵⁰ The two basic assumptions of the regression hypothesis are the existence of an equilibrium and a considerable (large) separation of time scales between the motion of the subsystem and that of the overall relaxation of the system.

The proof of the existence of an equilibrium in a system is more readily obtained through an analysis of the probability distribution $W(q, p; t)$ of the Brownian particles rather than the explicit trajectories calculated using the LE. The equation of motion for the distribution is the Fokker-Planck equation,¹

$$\begin{aligned}
\frac{\partial}{\partial t} W(q, p; t) &= \left\{ -\frac{\partial}{\partial q} p - \frac{\partial}{\partial p} [-V'(q) - \gamma_0 \psi^2(t)p] \right. \\
&\quad \left. - + \frac{\partial^2}{\partial p^2} \frac{\gamma}{\beta} \psi^2(t) \right\} W(q, p; t), \quad (\text{B1})
\end{aligned}$$

which corresponds to the nonstationary LE in Eq. 7. A direct substitution of the Boltzmann distribution confirms that it is indeed a solution of this equation. From this one can deduce that the Boltzmann distribution is the equilibrium distribution for systems with time-dependent friction. It might seem strange that equilibrium doesn't change when the system is driven by a time-dependent forcing friction. The key point is that the force is coupled only to the bath. The bath is taken to be infinite dimensional and absorbed the energy extract by the force. This, of course, does not mean that the system dynamics is not modified. On the contrary, as has been shown in the article, the diffusivity and reaction rates are modified by the periodicity of the externally driven friction. The time scales relevant to the second assumption are the period τ_f of the external force, the transient time τ_s of the system, the typical escape time τ_e of a thermal particle and the observation time τ . By construction of the naive model and the choice of its parameterization, these times follow the simple inequality: $(\tau_f \text{ or } \tau_s) \ll \tau \ll \tau_e$. As such, the system necessarily satisfies both of the assumptions needed to apply the Onsager hypothesis.

The rate constants may be obtained from a first order

master equation representing the population dynamics,

$$\dot{n}_a(t) = -k^+(t)n_a(t) + k^-(t)n_c(t) \quad (\text{B2a})$$

$$\dot{n}_c(t) = k^+(t)n_a(t) - k^-(t)n_c(t), \quad (\text{B2b})$$

where n_a (n_c) is the population of the left (right) well of the quartic potential in Eq. 17. The nonstandard feature is that the forward (backward) coefficient rate $k^\pm(t)$ is time dependent. As described in the text, they do have the same periodicity as the time-dependent friction. The master equation in Eq. B2 can be integrated in the usual manner to obtain the result,

$$\frac{\Delta n_a(t)}{\Delta n_a(t_0)} = e^{-\int_{t_0}^t \lambda(t') dt'}, \quad (\text{B3})$$

where $\Delta n_a(t)$ is the fluctuation of the momentary population of the left well relative to the equilibrium population of the well, and $\lambda \equiv (k^+ + k^-)$ as in the text. The Onsager regression hypothesis enables the connection to the equilibrium averaged expression,

$$\frac{\langle \delta\theta[q(t_0)]\delta\theta[q(t)] \rangle}{\langle \delta\theta[q(t_0)]^2 \rangle} = e^{\int_{t_0}^t -\lambda(t') dt'}. \quad (\text{B4})$$

Taking the time derivative of both sides leads to

$$\frac{\langle \delta\theta[q(t_0)]\dot{\delta\theta}[q(t)] \rangle}{\langle \delta\theta[q(t_0)]^2 \rangle} = -\lambda(t)e^{-\int_{t_0}^t \lambda(t') dt'} \quad (\text{B5a})$$

$$\approx -\lambda(t). \quad (\text{B5b})$$

The last equality is a result of the large time scale separation. So far there is no real difference from the standard

derivation. In the usual derivation, the assumption of stationarity would now permit the modification of the numerator into the form of a flux correlation function. This cannot be performed in the present time-dependent case. However, stationarity can be regained in this system by averaging over the period of the time-dependent friction. In practice, this can be achieved by initiating the subsystem at various time shifts τ relative to some arbitrary time origin in the time-dependent friction. An integration over the period of B5 leads to the averaged form of the reactive flux,

$$\frac{\omega}{2\pi} \int_0^{\frac{2\pi}{\omega}} d\tau \frac{\langle \delta q[\tau] \dot{q}[\tau] \theta[q(t+\tau)] \rangle}{\langle \delta\theta[q(\tau)]^2 \rangle} = \frac{\omega}{2\pi} \int_0^{\frac{2\pi}{\omega}} d\tau \frac{\langle \delta\theta[q(\tau)] \dot{\theta}[q(t+\tau)] \rangle}{\langle \delta\theta[q(\tau)]^2 \rangle} \quad (\text{B6a})$$

$$\approx \frac{\omega}{2\pi} \int_0^{\frac{2\pi}{\omega}} d\tau \lambda(\tau) \quad (\text{B6b})$$

$$\equiv -\bar{\lambda} \quad (\text{B6c})$$

The bar in the definition of $\bar{\lambda}$ indicates the average over time period of the time-dependent friction. Equation B6 is the averaged reactive flux rate for the nonstationary system with periodic friction. The above algebra also justifies the extension of the Melnikov-Meshkov theory to the time dependent friction case averaged over a period of the external perturbation described in Sec. VB.

* Present address: Department of Electrical and Computer Engineering, Georgia Institute of Technology, Atlanta GA; Electronic address: eli@bme.gatech.edu
 † Electronic address: heernandez@chemistry.gatech.edu
¹ H. Risken, *The Fokker-Planck Equation* (Springer-Verlag, New York, 1989).
² P. Hänggi, P. Talkner, and M. Borkovec, *Rev. Mod. Phys.* **62**, 251 (1990), and references therein.
³ H. Yang, Z. Zhuo, X. Wu, and X. Tang, *Phys. Lett A* **203**, 157 (1995).
⁴ H. W. Y. Hsia, N. Fang, and X. Lee, *Phys. Lett A* **215**, 326 (1996).
⁵ A. N. Drozdov and S. C. Tucker, *J. Phys. Chem. B* **105**, 6675 (2001).
⁶ A. N. Drozdov and S. C. Tucker, *J. Chem. Phys.* **114**, 4912 (2001).
⁷ K. R. Harris, *J. Chem. Phys.* **116**, 6379 (2002).
⁸ A. N. Drozdov and S. C. Tucker, *J. Chem. Phys.* **116**, 6381 (2002).
⁹ R. Hernandez and F. L. Somer, *J. Phys. Chem. B* **103**, 1064 (1999).
¹⁰ P. G. deGennes and J. Prost, *The Physics of Liquid Crystals* (Clarendon Press, Oxford, 1993).
¹¹ A. C. Diogo, *Mol. Cryst. Liq. Cryst.* **100**, 153 (1983).

¹² R. W. Ruhwandl and E. M. Terentjev, *Phys. Rev. E* **54**, 5204 (1996).
¹³ E. Hershkovitz and R. Hernandez, *J. Phys. Chem. A* **105**, 2687 (2001).
¹⁴ J. Christoph, P. Gabriel, and P. Davidson, *Adv. Mater.* **12**, 9 (2000).
¹⁵ G. Srajer, S. Fraden, and R. Meyer, *Phys. Rev. A* **39**, 4828 (1989).
¹⁶ F. Brochard, *J. Phys. (Paris) Lett.* **35**, L19 (1974).
¹⁷ K. B. Migler and R. Meyer, *Phys. Rev. E* **48**, 1218 (1993).
¹⁸ V. Roman and E. Terent'ev, *Colloid J. USSR* **51**, 435 (1989).
¹⁹ V. I. Mel'nikov and S. V. Meshkov, *J. Chem. Phys.* **85**, 1018 (1986).
²⁰ E. Pollak, H. Grabert, and P. Hänggi, *J. Chem. Phys.* **91**, 4073 (1989).
²¹ J. S. Langer, *Ann. Phys. (NY)* **54**, 258 (1969).
²² B. J. Matkowski, Z. Schuss, and E. Ben-Jacob, *SIAM (Soc. Ind. Appl. Math.) J. Appl. Math.* **42**, 835 (1982).
²³ B. J. Matkowski, Z. Schuss, and C. Tier, *SIAM (Soc. Ind. Appl. Math.) J. Appl. Math.* **43**, 673 (1983).
²⁴ B. Berne, *Chem. Phys. Lett.* **107**, 131 (1984).
²⁵ M. Borkovec and B. Berne, *J. Chem. Phys.* **82**, 794 (1985).
²⁶ A. Nitzan, *Adv. Chem. Phys.* **70**, 489 (1988).

- ²⁷ E. Hershkovitz and E. Pollak, *J. Chem. Phys.* **106**, 7678 (1997).
- ²⁸ R. Benzi, A. Suter, and A. Vulpiani, *J. Phys. A* **14**, L453 (1981).
- ²⁹ L. Gammaitoni, P. Hänggi, P. Jung, and F. Marchesoni, *Rev. Mod. Phys.* **70**, 223 (1998).
- ³⁰ C. R. Doering and J. C. Gadoua, *Phys. Rev. Lett.* **69**, 2318 (1992).
- ³¹ P. Reimann and P. Hänggi, in *Stochastic Dynamics*, Vol. 484 of *Lecture Notes in Physics*, edited by L. Schimansky-Geier and T. Poschel (Springer, Berlin, 1997), pp. 127–139.
- ³² J. Lehmann, P. Reimann, and P. Hänggi, *Phys. Rev. Lett.* **84**, 1639 (2000).
- ³³ M. O. Magnasco, *Phys. Rev. Lett.* **71**, 1477 (1993).
- ³⁴ P. Reimann, *Phys. Rep.* **361**, 57 (2002).
- ³⁵ A. Engel, H. W. Mueller, P. Reimann, and A. Jung, *Phys. Rev. Lett.* **91**, 060602 (2003).
- ³⁶ R. F. Grote and J. T. Hynes, *J. Chem. Phys.* **73**, 2715 (1980).
- ³⁷ P. Hänggi and F. Mojtabai, *Phys. Rev. A* **26**, 1168 (1982).
- ³⁸ B. Carmeli and A. Nitzan, *Phys. Rev. Lett.* **49**, 423 (1982).
- ³⁹ R. Hernandez and F. L. Somer, *J. Phys. Chem. B* **103**, 1070 (1999).
- ⁴⁰ F. L. Somer and R. Hernandez, *J. Phys. Chem. B* **104**, 3456 (2000).
- ⁴¹ G. R. Haynes, G. A. Voth, and E. Pollak, *J. Chem. Phys.* **101**, 7811 (1994).
- ⁴² E. Hershkovitz, *J. Chem. Phys.* **108**, 9253 (1998).
- ⁴³ D. Chandler, *J. Chem. Phys.* **68**, 2959 (1978).
- ⁴⁴ A. M. Frishman and E. Pollak, *J. Chem. Phys.* **98**, 9532 (1993).
- ⁴⁵ E. Pollak, *J. Chem. Phys.* **85**, 865 (1986).
- ⁴⁶ R. Hernandez, *J. Chem. Phys.* **110**, 7701 (1999).
- ⁴⁷ P. E. Kloeden and E. Platen, *Numerical Solution of Stochastic Differential Equations* (Springer-Verlag, New York, 1992).
- ⁴⁸ W. H. Press, B. P. Flannery, S. A. Teukolsky, and W. T. Vetterling, *Numerical Recipes* (Cambridge University Press, Cambridge, UK, 1988).
- ⁴⁹ M. P. Allen and D. J. Tildesley, *Computer Simulations of Liquids* (Oxford, New York, 1987).
- ⁵⁰ D. Chandler, *Introduction to Modern Statistical Mechanics* (Oxford University Press, New York, 1987).